Chemosphere 370 (2025) 143889

Contents lists available at ScienceDirect

Chemosphere

journal homepage: www.elsevier.com/locate/chemosphere

Kinetic and isotherm study for the adsorption of per- and polyfluoroalkyl substances (PFAS) on activated carbon in the low ng/L range

Marko Pranić [a], Livio Carlucci [a], Albert van der Wal [a,b], Jouke E. Dykstra [a,*]

[a] Environmental Technology, Wageningen University & Research, P.O. Box 17, 6700 AA Wageningen, The Netherlands
[b] Evides Water Company, P.O. Box 4472, 3006 AL Rotterdam, The Netherlands

HIGHLIGHTS

- PFAS adsorption experiments were performed at 0.1–100 ng/L.
- Pore size distribution of activated carbon determines PFAS adsorption.
- Significantly lower adsorption capacities were observed than previously reported.
- Surface diffusion model showed very low PFAS surface mobility.
- PFAS adsorption mechanism depends on PFAS concentrations.

GRAPHICAL ABSTRACT

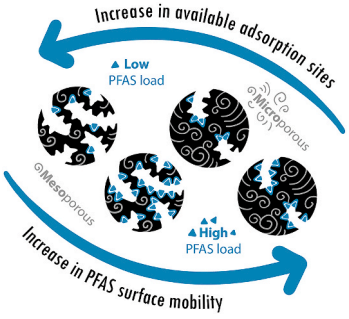

ARTICLE INFO

Keywords:
PFAS
Adsorption
Drinking water treatment
Surface diffusion

ABSTRACT

Activated carbon adsorption is a widely used technology for the removal of per- and polyfluoroalkyl substances (PFAS). However, the rapid breakthrough of PFAS in activated carbon filters poses a challenge to meet the very low allowable PFAS concentrations in drinking water, leading to high operational costs. In this study, we conducted batch isotherm and kinetic adsorption experiments using nine different types of PFAS molecules at concentrations typically found in water sources used for drinking water production (0.1–100 ng/L). The isotherm experiments at these low concentrations reveal that the maximum adsorption capacity of several PFAS is much lower than reported in literature. The estimated isotherms were included in a dynamic model that includes mass transport based on surface diffusion. This model effectively describes the experimental kinetic data, and the obtained surface diffusion coefficients indicate a very slow PFAS surface mobility. Additionally, our findings indicate that PFAS surface mobility decreases in scenarios with more available adsorption sites. Notably, mesoporous activated carbon, with its higher adsorption capacity, exhibits lower PFAS surface mobility than microporous carbon with lower PFAS adsorption capacity. Moreover, for both carbons, we observed a decrease in PFAS surface mobility at higher carbon loadings when the surface is less saturated with PFAS. Our findings suggest potential inherent limitations in activated carbon technology for PFAS removal under environmentally relevant conditions, as we observed lower adsorption capacities than previously reported at higher concentrations, and a decrease in PFAS surface mobility with more available adsorption sites.

* Corresponding author.
E-mail addresses: marko.pranic@wur.nl (M. Pranić), jouke.dykstra@wur.nl (J.E. Dykstra).

https://doi.org/10.1016/j.chemosphere.2024.143889
Received 4 May 2024; Received in revised form 17 September 2024; Accepted 2 December 2024
Available online 21 December 2024

1. Introduction

Per- and polyfluoroalkyl substances (PFAS) are persistent organic micropollutants of industrial origin that raise significant concerns due to their suspected toxicity at relatively low concentrations found in the environment (Buck et al., 2011; KEMI, 2015; Schrenk et al., 2020). In sources used for drinking water production, the sum of measured concentrations of PFAS commonly ranges from less than 1 ng/L to approximately 1 μg/L (Boone et al., 2019; Gebbink et al., 2017). The current EU directive set a total maximum concentration of 100 ng/L in drinking water for a selected group of PFAS of concern (The European Parliament and the Council of the European Union, 2020). A report by the European Food Safety Authority recommends that the total concentration of four listed PFAS components should not exceed 4.4 ng/L in drinking water (Schrenk et al., 2020), which has been adapted in a recent proposal for a new EU directive (The European Parliament and the Council of the European Union, 2022). Furthermore, the US EPA has recently announced new regulations for five PFAS of concern, with allowable concentrations ranging from 4 to 10 ng/L depending on the specific PFAS (US EPA, 2024).

Adsorption technology has been proven in reducing PFAS concentrations to acceptable levels in drinking water (Gagliano et al., 2020; Dixit et al., 2021a). Several studies demonstrated effective removal of PFAS using adsorptive media (Belkouteb et al., 2020; McNamara et al., 2018; Roest et al., 2021). However, these studies also reported relatively rapid breakthrough of PFAS in adsorption columns, meaning frequent adsorbent regeneration is needed to maintain performance. Considering that adsorbent regeneration significantly contributes to the total treatment costs, there is an economic interest to minimize the frequency of regeneration (Belkouteb et al., 2020).

Activated carbon (AC) is the primary adsorbent used in drinking water treatment, due to its cost-effectiveness, high affinity for various compounds, and large adsorption surface area (Worch, 2012). Sörengård et al. (2020) tested 44 different adsorbents for PFAS removal and found that ACs exhibited the highest performance. However, understanding which AC properties impact PFAS removal is crucial. A review by Liu et al. (2020) showed that PFAS removal improves with carbon materials that have fewer oxygen surface groups. Positively charged AC materials also delay PFAS breakthrough compared to neutral or negatively charged materials (Cantoni et al., 2021; Park et al., 2020). Furthermore, pore size distribution significantly impacts PFAS adsorption. Kancharla et al. (2022) reported that micropores (diameter <2 nm) enhance the adsorption of short-chain PFAS, while mesopores (>2 nm) are more crucial for the adsorption of long-chain PFAS. According to Du et al. (2014), mesopores provide sufficient space for the diffusion of relatively large long-chain PFAS that cannot easily enter the micropores.

Empirical kinetic models, such as the pseudo-first or pseudo-second order models, are frequently employed to describe the dynamics of PFAS adsorption (Dixit et al., 2021b; Yu et al., 2009, 2012). However, these models offer limited predictive value and lack physical interpretation. In contrast, mechanistic intraparticle diffusion models provide a more detailed description of mass transfer within AC granules. One example of such a model is the pore and surface diffusion model (PSDM) (Geankoplis and Leyva-Ramos, 1985; Souza et al., 2017). The PSDM model offers the advantage of obtaining diffusion coefficients that can be used to predict PFAS breakthrough curves, and can thereby support the design of AC filters for PFAS removal in pilot and full-scale treatment plants (Burkhardt et al., 2022). Additionally, diffusion coefficients can be correlated with molecular properties, further enhancing the understanding of the adsorption process (Piai et al., 2019).

To investigate the interactions between PFAS and adsorbents, adsorption experiments are often conducted using high PFAS concentrations and large adsorbent quantities. However, these conditions do not accurately represent realistic conditions in drinking water treatment (Gagliano et al., 2020). Furthermore, the mechanisms responsible for adsorption of micropollutants can vary with concentration (Kaur et al., 2018; Gong et al., 2021). Specifically, for surfactants such as PFAS, high concentrations (>20 mg/L) can lead to the formation of (hemi-)micelles (Yu et al., 2009). A study by Zaggia et al. (2016) demonstrated the possible formation of molecular aggregates for long-chain PFAS at a concentration of 1 mg/L, a level not typically observed in drinking water treatment. Several studies conducting PFAS experiments at concentrations <100 ng/L were conducted in pilot or full-scale systems, focusing solely on obtaining breakthrough curves (Belkouteb et al., 2020; Burkhardt et al., 2022; Chow et al., 2022; Liu et al., 2019). Adsorption isotherms for PFAS in the 0.1–100 ng/L concentration range have not been systematically reported in experimental studies. Consequently, drawing conclusions regarding adsorption mechanisms and capacities at such low concentrations is challenging. Furthermore, the lack of isotherm data significantly limits modelling of adsorption systems using mechanistic models.

In this study, batch adsorption experiments are performed to investigate the mechanisms of PFAS adsorption within concentration ranges relevant to drinking water treatment. To our knowledge, this is the first study to report isotherm and kinetic data for PFAS adsorption in the 0.1–100 ng/L range. We obtain isotherm parameters and intraparticle diffusion coefficients for nine PFAS compounds using two types of AC with distinct pore size distributions. The selected ACs have similar surface charge properties, allowing us to isolate and clarify the effects of pore size distribution on PFAS adsorption. The PFAS compounds are selected for their relevance to drinking water treatment regulations and their molecular properties, to provide insight into their interactions with microporous and mesoporous AC. This study aims to asses whether there are significant differences between the isotherm and kinetic parameters derived from our novel low-concentration data and those widely reported in the literature, which are based on higher concentrations. Accurate isotherm and kinetic parameters are essential for predicting and designing effective adsorption filters. To ensure that any deviations between our results in the 0.1–100 ng/L range and the higher concentrations reported in the literature are not due to experimental artifacts, we conducted additional experiments on perfluorooctanoic acid (PFOA) within the 1–1000 μg/L range commonly studied.

2. Materials and methods

2.1. Activated carbons

Two granular activated carbons (GAC) with distinct pore size distributions were selected for this study. The carbon selected for its higher micropore volume and micropore surface area is AquaSorb^{TM} K-CS from Jacobi (CS), which is a thermally activated coconut shell-based activated carbon. The carbon selected for its higher mesopore volume and mesopore surface area is SRD from Chemviron, which is a reagglomerated bituminous-based activated carbon. According to the supplier, SRD possesses similar properties to the commonly used Filtrasorb F400, but with higher mesopore volume, which was also confirmed by our N_2 physisorption analysis (see Figure S.1). The GAC particles were sieved to obtain a diameter range of 0.60–0.85 mm, which aligns with the dominant particle sizes used in some activated carbon filters (Cantoni et al., 2021). A narrow particle size distribution was selected to ensure particles homogeneity. After sieving, the particles were thoroughly washed with demineralized water, and were then dried and stored. Prior to the adsorption experiments, the GAC was dried at 105 °C for 24 h to eliminate moisture. The GAC was then weighed, boiled to remove entrapped air, and subsequently cooled down to room temperature. Several well-established methods were performed to determine the properties of GAC (Ateia et al., 2020), and the results are summarized in Table S.1.

2.2. PFAS

Nine PFAS compounds were selected for this study. Molecular properties of these PFAS can be found in Table 1. The selected PFAS represent a combination of short-chain and long-chain compounds, encompassing PFAS with either sulfonic or carboxylic functional groups, as well as perfluorooctane sulfonamide acid (FOSA), which possesses an sulfonamide functional group. Most of the selected PFAS compounds were included duo to their regulatory maximum concentrations limits, while FOSA was selected to explore the impact of functional groups on adsorption.

2.3. Adsorption experiments

Isotherm and kinetic adsorption experiments started by adding a specific quantity of activated carbons to a 1 L solutions containing mixture of 9 PFAS compounds dissolved in Mili-Q water, buffered at pH 7.2 using a 10 mM phosphate buffer (5 mM of Na_2HPO_4 + 5 mM KH_2PO_4). This was the minimum buffer concentration required to maintain a constant pH throughout the experiment in all bottles. The initial concentration of the PFAS compounds was similar in all experiments, ranging from ~70 to ~100 ng/L depending on the specific PFAS. The experiments were conducted in polypropylene copolymer (PPCO) bottles, which were placed horizontally on an orbital shaker and agitated at 150 rpm at a temperature of ~20 °C. Each reported datapoint was obtained by sacrificing the entire batch volume, taking a ~350 mL water sample that was stored at 4 °C in PP bottles for a maximum of two weeks before analysis. Notably, a batch volume of 1 L was used, which exceeds the typical volumes for batch adsorption experiments, to minimize experimental errors in the ng/L concentration range.

In the kinetic experiments, PFAS concentrations in solution were monitored for up to 40 days for both types of GAC, using loadings of 5 mg/L, which is a typical carbon loading in drinking water treatment (Ateia et al., 2020), and of 100 mg/L, which reflects a scenario with an excess of adsorption sites. Adsorption equilibrium was reached for all PFAS compounds. Initially, during the period of most rapid kinetic changes, samples were taken at shorter intervals (every few hours), and subsequently at longer intervals (every few days). To evaluate PFAS adsorption onto the experimental PPCO and storage PP bottle, a kinetic control experiment was conducted without GAC. No significant PFAS adsorption on the bottles was observed, and the resulting kinetic curves are shown in Figure S.3.

To obtain adsorption isotherms, activated carbon loading was varied between 2 and 500 mg/L. These doses were chosen based on recommendations in Worch (2012) to reduce experimental errors in isotherm determination. All samples were collected after 40 days, once adsorption equilibrium had been reached. The adsorbent loading is evaluated by

$$q_{eq} = \frac{V_l}{m_a}\left(c_0 - c_{eq}\right) \quad (1)$$

in which q_{eq} is the adsorbent loading in equilibrium (ng_{PFAS}/mg_{GAC}), V_l is the volume of the bulk solution (L), m_a is the mass of dry activated carbon, c_0 is the starting PFAS concentration in the bulk solution, and c_{eq} is the concentration in equilibrium.

Our study aims to identify potential differences between high-concentration PFAS adsorption data reported in the literature and our novel low ng/L data. To ensure these differences are not due to experimental artifacts, we conducted isotherm experiments with PFOA at higher concentrations. PFOA was selected because it is one of the most extensively studied PFAS compounds. The isotherm experiments at elevated starting concentrations (1–1000 μg/L) followed the same procedures as described earlier in this section. Detailed experimental procedure is provided in Section 2 of the Supplementary Information (S.I.).

2.4. Determination of PFAS concentrations

The PFAS samples, obtained from experiments with starting concentrations up to 100 ng/L, were analysed at the certified analytical lab AquaLab Zuid B.V. (The Netherlands) using the Xevo TQ-XS LC-MS coupled with an Acquity UPLC CSH Phenyl-Hexyl column. The quantification limits for the analysed PFAS ranged from 0.1 to 0.5 ng/L. For the PFOA isotherm experiments, which had starting concentrations between 1 and 1000 μg/L, analysis was carried out using the SCIEX 5500+ LC-AD30 system, with a Phenomenex Kinetex C18 column. The quantification limit for PFOA was 2.5 ng/L. Additional details on PFAS detection and analysis methodologies are provided in Section 3 of the S.I.

3. Results and discussion

Equilibrium adsorption data for nine different PFAS at environmentally relevant concentrations (0.1–100 ng/L) were collected using two activated carbons with contrasting pore size distributions: the more microporous CS and the more mesoporous SRD (Table S1) To describe and analyse the PFAS equilibrium data, three widely used isotherm models, i.e., the linear, Langmuir and Freundlich models (Table S.7), were applied and the results are discussed in Section 3.1. Isotherm parameters were estimated based on non-linear regression. The fitting

Table 1
PFAS properties and estimated values of isotherm parameters for granular activated carbons used in this study.

			PFBS	PFHxS	PFOS	PFDS	PFPeA	PFOA	PFNA	FOSA	GenX
PFAS properties	Chain length		4	6	8	10	4	8	9	8	5
	Functional group		SO_3^-	SO_3^-	SO_3^-	SO_3^-	COO^-	COO^-	COO^-	SO_2NH_2	COO^-
	Mw (g/mol)		299	399	499	599	264	414	464	499	329
	LogK_{ow} [a]		1.82	3.16	4.49	6.83	3.01	4.81	5.48	5.8	4
	pK_a [a]		−3.31	0.14	<1.0	−3.24	0.34	<4.2	−0.21	3.37	3.8
GAC	Isotherm	Parameter[b]									
SRD (mesoporous)	Linear	a	3.77	4.54	5.07	8.23	0.73	3.86	4.06	10.72	1.21
	Langmuir	q_{max}	63.93		not available		47.67	not available		96.77	63.61
		K_L	0.074				0.020			0.137	0.024
	Freundlich	K_f	5.71	6.50	8.42	10.27	1.57	5.06	5.04	11.46	2.36
		n	0.63	0.86	0.76	0.84	0.70	0.87	0.90	0.75	0.70
CS (microporous)	Langmuir	q_{max}	11.23	11.30	12.93	7.09	9.48	10.35	13.19	16.07	8.27
		K_L	0.099	0.157	0.086	0.401	0.023	0.251	0.093	0.089	0.075
	Freundlich	K_f	1.92	3.48	2.70	1.34	0.47	3.10	2.60	2.46	1.29
		n	0.41	0.25	0.36	0.53	0.60	0.31	0.38	0.46	0.40

[a] For GenX information obtained from Vakili et al. (2021), and for other PFAS from Gagliano et al. (2020)
[b] Units of parameters are: a (L/mg); q_{max} (ng/mg); K_L (L/ng); K_f (ng/mg)/(ng/L)^n; R^2 for estimated isotherms ranges from 0.86 to 0.99 and can be found in Table S8.

results of the isotherm parameters were evaluated using least squares fit statistical analysis.

3.1. Adsorption isotherms

Our findings indicate that, for an initial PFAS concentration of ~100 ng/L, the adsorption equilibrium of the PFAS compounds included in this study can be accurately described by linear isotherms for mesoporous granular activated carbon (GAC) such as SRD. Conversely, the adsorption equilibrium of PFAS on microporous GAC, such as CS, is better described by Langmuir isotherms. In addition to linear isotherms, Langmuir isotherms effectively capture the adsorption of short-chain PFAS on SRD (Fig. 1). The Freundlich isotherm model also describes adsorption on both types of GAC, but because of its empirical nature, these results are not discussed in detail in this manuscript.

The estimated isotherm parameters are provided in Table 1. Fig. 1 shows the isotherm curves for selected PFAS compounds, while the isotherm curves for other components can be found in Figure S.5, and S.6.

3.1.1. Comparison of 0.1–100 ng/L PFAS isotherm parameters with literature values

For mesoporous SRD, the adsorption data can be described with a linear isotherm (Fig. 1), most likely, because of the high adsorption capacity. Consequently, for the low initial PFAS concentrations used in our experiments, the carbon surface was not nearing saturation, allowing the linear isotherm to accurately describe the data. For experiments at higher PFAS concentrations (0.1 mg/L and 1 mg/L) Langmuir maximum loadings were observed for SRD (see Section 3.3), similar to the findings of Ochoa-Herrera and Sierra-Alvarez (2008), who reported results using mesoporous F400, a carbon with a comparable pore size distribution to SRD. Notably, Ochoa-Herrera and Sierra-Alvarez (2008) conducted their experiments in the mg/L range. Additionally, a literature review conducted by Gagliano et al. (2020) reported 12 studies where Langmuir adsorption isotherms were observed for GAC adsorption of PFAS at starting concentrations in the µg/L or mg/L range.

For microporous CS, the adsorption can be described with a Langmuir isotherm (Fig. 1), and it is worth noting that the K_L and q_{max} values reported in this study for PFAS adsorption on activated carbon are significantly different from those reported in other studies that use Langmuir isotherms. In our study, K_L values range from 0.02 to 0.25 L/ng, while q_{max} values range from 8 to 97 ng/mg. High values of K_L and low values of q_{max} indicate a specific and localized adsorption. In contrast, Ochoa-Herrera and Sierra-Alvarez (2008) reported K_L values ranging from $3{\cdot}10^{-8}$ to $1.3{\cdot}10^{-7}$ L/ng and q_{max} values ranging from $99{\cdot}10^{3}$ to $2.36{\cdot}10^{5}$ ng/mg. Similarly, Inyang and Dickenson (2017) reported K_L values ranging from $3.1{\cdot}10^{-7}$ to $5.2{\cdot}10^{-7}$ L/ng, and q_{max} ranging from $28{\cdot}10^{3}$ to $41{\cdot}10^{3}$ ng/mg, while Du et al. (2015) reported K_L values ranging from $3.2{\cdot}10^{-4}$ to $1.6{\cdot}10^{-3}$ L/ng, and q_{max} values ranging from $18{\cdot}10^{3}$ to $4.26{\cdot}10^{5}$ ng/mg.

The significant discrepancies between our isotherm data and literature values can largely be attributed to the difference in concentration ranges used in the experiments. Our study employed a lower PFAS concentration to carbon ratio than other studies, raising the question of which isotherm parameters are most practical and valuable for designing activated carbon filters, particularly in predicting breakthrough curves. To predict these breakthrough curves, diffusion

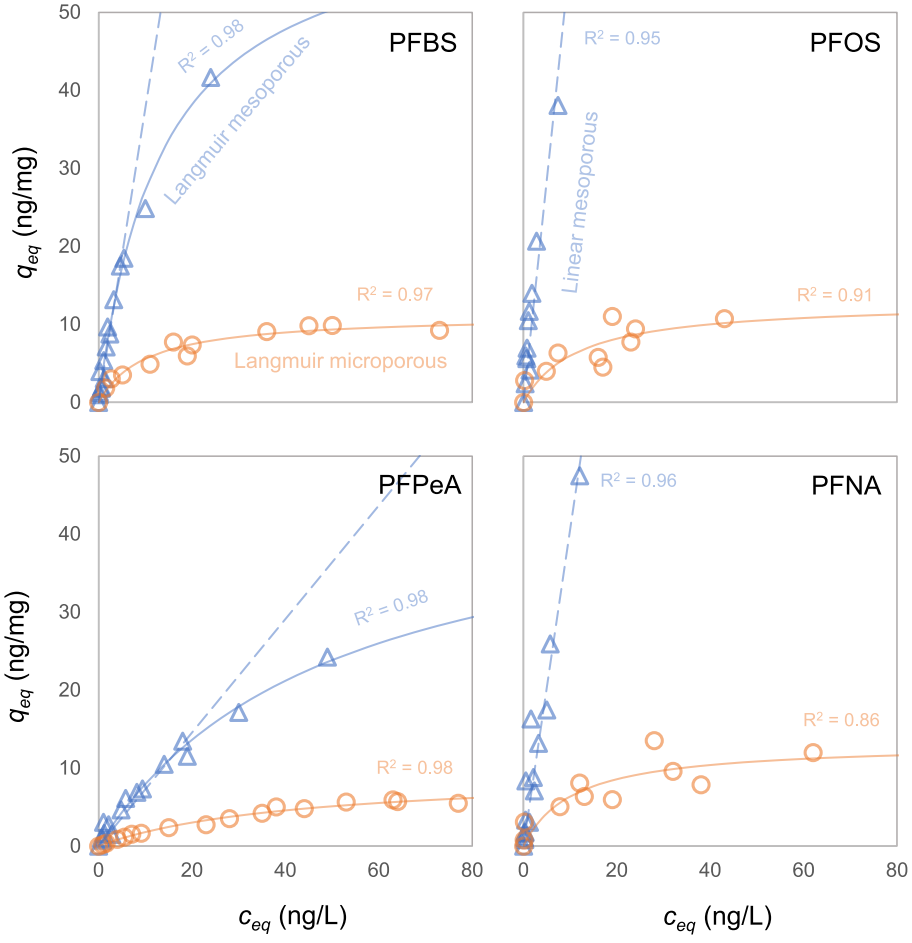

Fig. 1. Experimental data for the adsorption of PFBS, PFOS, PFPeA and PFNA on two activated carbons, SRD (blue triangles) and CS (orange circles), described with Langmuir (full line) and linear (dashed line) isotherms.

coefficients are also required (Worch, 2012; Burkhardt et al., 2022), and these values vary significantly between high and low PFAS concentrations. These findings are discussed in detail in Section 3.3. For drinking water systems with PFAS concentrations <100 ng/L, as examined in this study, our isotherms are likely more relevant and practical. Conversely, for systems treating water with higher PFAS concentrations, such as industrial wastewaters, the isotherms reported in literature may be more applicable.

3.1.2. Impact of pore size distribution on 0.1–100 ng/L PFAS isotherm parameters

In the case of PFAS adsorption on mesoporous SRD, we have observed a linear relationship between the parameter $a(L/mg)$ (also known as distribution coefficient, K_D (Ateia et al., 2020)) of the linear isotherm and the number of fluorinated carbons present in the PFAS chain, as depicted in Fig. 2. This correlation demonstrates that PFAS adsorption increases with chain length, indicating that longer-chain PFAS exhibit higher affinity for adsorption. Numerous studies have reported better adsorption of long-chain PFAS compared to short-chain PFAS (Sörengård et al., 2020; Franke et al., 2019; Wu et al., 2020; Qiu et al., 2007)[-](Sörengård et al., 2020; Franke et al., 2019; Wu et al., 2020; Qiu et al., 2007), attributing this observation to hydrophobic effects. These effects intensify with increasing chain length, leading to enhanced interaction between PFAS and the hydrophobic carbon surface. In addition to chain length, the functional group of PFAS also exhibits an influence on the adsorption on SRD. Fig. 2 illustrates that PFAS compounds with sulfonic functional groups (PFSAs) demonstrate higher adsorption compared to those with carboxylic functional groups (PFCAs) for the same number of fluorinated carbons. The difference in adsorption between PFSAs and PFCA, consistently reported in literature (Gagliano et al., 2020), is attributed to the larger and less soluble sulfonic group in PFSAs, compared to the carboxylic group in PFCAs, for the same number of fluorinated carbons (Higgins and Luthy, 2007). Furthermore, Fig. 2 shows that FOSA, which has the lowest water solubility of the studied PFAS, because of its uncharged sulfonamide head group (Ahrens, 2011), exhibited the highest adsorption on SRD. A study by Sörengård et al. (2020) on 44 adsorbents also observed a decreasing trend in adsorption as follows: FOSA > PFSAs > PFCAs.

As discussed in the previous paragraph, we observed the influence of functional groups and carbon chain length on PFAS adsorption on mesoporous carbon at low ng/L concentrations, which is consistent with findings from existing studies at higher concentrations. Contrary to findings reported in literature, this correlation was not observed for microporous CS. The adsorption of PFAS on CS can be described using the Langmuir isotherm model (Fig. 1). However, we did not observe a pronounced dependence of the Langmuir parameters on the specific properties of PFAS. This can be explained by the fact that long-chain PFAS, with the Stokes radius of ~0.4–0.6 nm (Li et al., 2021), cannot easily enter the micropores (<1 nm radius) of activated carbon. Therefore, increasing the fluorinated carbon chain length does not necessarily enhance adsorption, contrary to observations for mesoporous SRD (Fig. 2). Furthermore, nanobubbles have been suggested as a mechanism that may facilitate the transport of hydrophobic PFAS towards the carbon surface (Yuan et al., 2023). Since nanobubbles at the surface are typically 10–80 nm in height (Atkinson et al., 2019), carbon materials with more mesopores could potentially accommodate a greater number of nanobubbles, thereby improving the adsorption process. At low PFAS concentrations, micropores in CS may pose a limiting factor for adsorption, whereas mesopores in SRD provide sufficient space, making PFAS characteristics more significant in determining the adsorption equilibrium.

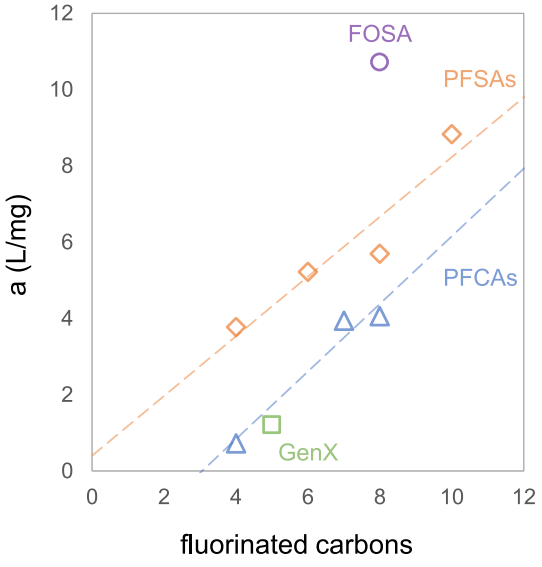

Fig. 2. Relationship between the linear isotherm parameter a (L/mg) and the number of fluorinated carbons in the PFAS chain for adsorption on SRD activated carbon. The datapoints in the figure represent carboxylic PFAS (blue triangles), sulfonic PFAS (orange diamonds), GenX (green square), and FOSA (purple circle).

Further evidence highlighting the crucial role of mesopores in PFAS adsorption in the ng/L range is based on comparing the Langmuir parameters between CS and SRD. The Langmuir parameter K_L, which represents the adsorbate's affinity for the adsorbent, shows comparable values for PFBS, PFPeA, FOSA, and GenX, while the maximum adsorption capacity (q_{max}) is consistently higher for SRD compared to CS (see Table 1). This intriguing finding suggests, despite having similar affinities SRD has a higher capacity to adsorb PFAS than CS. SRD's enhanced PFAS adsorption capacity is likely not due to electrostatic interactions, given the low concentration of acidic surface groups, and minimal positive charge at the experimental pH of ~7 for both carbons (see Table S1). Instead it can be attributed to SRD's larger mesopore surface area (142 m^2/g for SRD vs 48 m^2/g for CS). Our findings are in agreement with previous studies demonstrating that mesoporous adsorbents exhibit better removal of larger PFAS molecules compared to microporous adsorbents (Zaggia et al., 2016; Du et al., 2015; Appleman et al., 2013). Contrary to previous speculation that PFAS adsorption on activated carbon could be hindered by competition with organic matter or other PFAS, our study conducted in a 10 mM phosphate buffer matrix resembling the conductivity of drinking water (~800 μs/cm), demonstrate that, PFAS adsorption is inherently limited on microporous carbon, even in simplified matrices.

3.2. Kinetic experiments

Kinetic adsorption experiments were conducted using two types of granular activated carbon, namely mesoporous SRD and microporous CS, at two different carbon loadings (5 mg/L and 100 mg/L), with a mixture of 9 PFAS with initial concentration of ~70–100 ng/L. The kinetic data were described using diffusion models, which are detailed in Section 5 of S.I. The kinetic data showed good agreement with the homogenous surface diffusion model (HSDM) and the pore diffusion model (PDM). For both models, fitting was performed with and without considering film diffusion, and the effect of film diffusion was negligible, see Section 7.1 of S.I. Since linear isotherms were able to describe the adsorption on SRD, and the Langmuir isotherm was suitable for CS, their respective parameters were used as input for the diffusion models. The results obtained from the HSDM model are presented and discussed in Section 3.2.1. The results obtained from the PDM model are discussed in Section 7.2 of S.I. as estimated values of pore diffusion coefficients were mostly found to be unrealistic.

3.2.1. Surface diffusion

The experimental kinetic data was analysed using the HSDM model,

with the surface diffusion coefficient, D_s, as fitting parameter. The data was described very well, and R^2 was in most cases higher than 0.93 as reported in Table S.14. Since for PFDS low values of R^2 were obtained, PFDS data is reported in S.I. but not discussed in manuscript. The results of the fitting procedure for PFPeA and PFNA are presented in Fig. 3, while the other results are in Figures S.10. and S.11. The estimated values of D_s for all PFAS are reported in Table S14.

The surface diffusion model describes the mechanism through which adsorbates, in their adsorbed state, are transported along the internal surface of adsorbent particles (Do et al., 2001). The diffusion process is governed by the surface diffusion coefficient, D_s, which is influenced by adsorption strength between the surface and adsorbent, concentration of adsorbate in adsorbed state, the temperature, and the molecular weight of the adsorbate (Worch, 2012). As explained by Worch (2012), a higher adsorption strength leads to reduced adsorbate mobility, i.e., more strongly adsorbed molecules are less mobile. The adsorption strength can be characterized by the Freundlich coefficient, K_f, listed in Table 1. Higher K_f values correspond to stronger adsorption, which in turn leads to increased adsorbent loadings (Worch, 2012).

Fig. 4a highlights the significance of adsorption strength on diffusion. It is evident that, at a carbon loading of 5 mg/L, the values of D_s (surface mobility) for PFAS adsorption on CS are consistently higher than those for SRD. This observation indicates that CS exhibits faster PFAS surface mobility compared to SRD, which can be attributed to the lower adsorption strength of PFAS towards CS, as supported by the K_f values (Table 1), which are several times lower for CS compared to SRD. The only exception is that for a carbon loading of 100 mg/L, D_s of short-chain PFAS is higher for SRD than for CS (Fig. 4b). This can be explained by the occurrence of pore diffusion in addition to surface diffusion. As discussed in Section 7.2. of the S.I. the pore diffusion model yielded realistic values for PFAS adsorption on SRD at a carbon loading of 100 mg/L, while it was not effective for other cases. The pore diffusion model is known to accurately describe the transport of hydrophilic compounds (Piai et al., 2019), and short-chain PFAS are considered hydrophilic in nature.

The dependence of D_s on surface adsorbate concentration can occur in the case of heterogenous adsorbents like AC that have adsorption sites of different energy (Worch, 2012; Do et al., 2001). During the adsorption process, there is a progressive filling of adsorption sites, beginning with those of higher energy and gradually moving to sites with lower energy (Gilliland et al., 1974). Consequently, there is a decrease in adsorption energy, and an increase in adsorbate mobility as the concentration of adsorbed species increases (Neretnieks, 1976a). From the results in this study, the dependence of D_s on surface adsorbent concentration follows from Fig. 4, when comparing the values of D_s for 5 mg/L and 100 mg/L carbon loadings, for the same AC. For most cases in Fig. 4, the surface diffusion coefficient is higher at a lower carbon loading, when the surface is more saturated with PFAS, i.e., when the surface interactions during intraparticle transport are considered to be weaker. Previous studies have demonstrated a relation between adsorption energy, surface adsorbent concentration, and adsorbent mobility, with higher D_s values observed when the surface is more saturated with adsorbent (Do et al., 2001; Gilliland et al., 1974; Neretnieks, 1976a; Suzuki and Takao, 1982; Leyva-ramos, 2013; Neretnieks, 1976b). It is important to note that while the surface diffusion coefficient may be higher at lower carbon loadings, overall PFAS removal is still faster at higher carbon

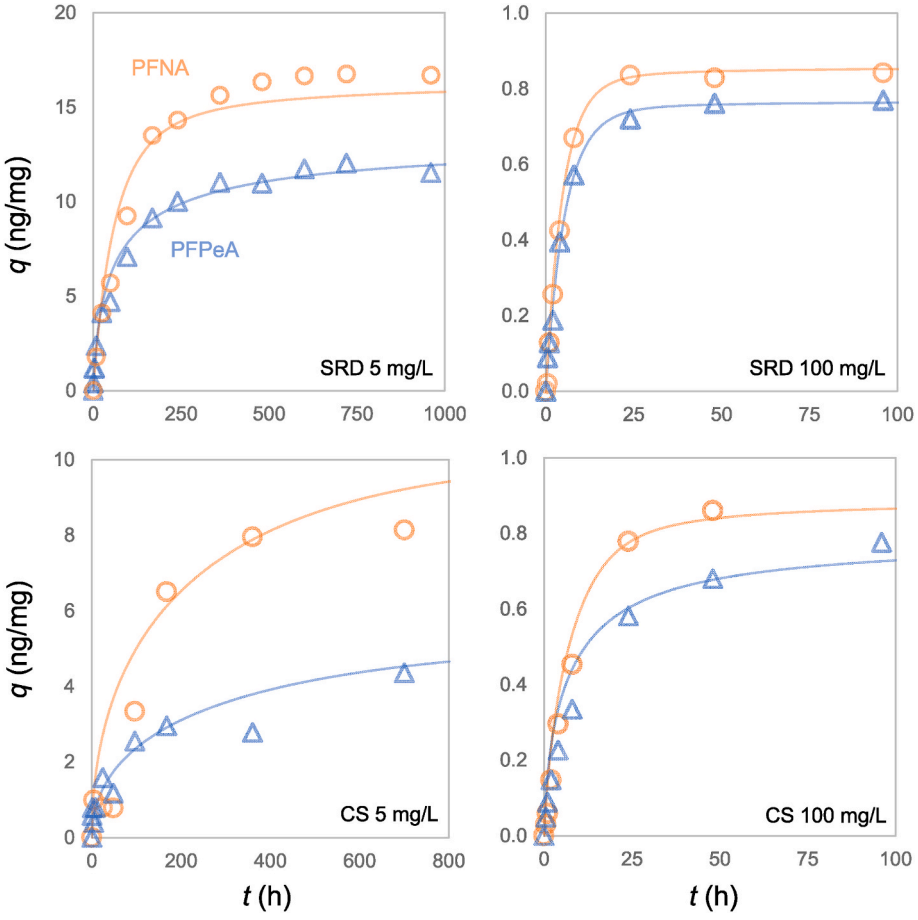

Fig. 3. Adsorbate loading, q (ng/mg), of PFNA and PFPeA as a function of time for different loadings of mesoporous SRD (5 and 100 mg/L) and microporous CS (5 and 100 mg/L). Experimental data is represented by blue triangles for PFPeA and orange circles for PFNA. Theoretical predictions, based on the HSDM model, are depicted by solid lines, with blue indicating PFPeA, and orange PFNA.

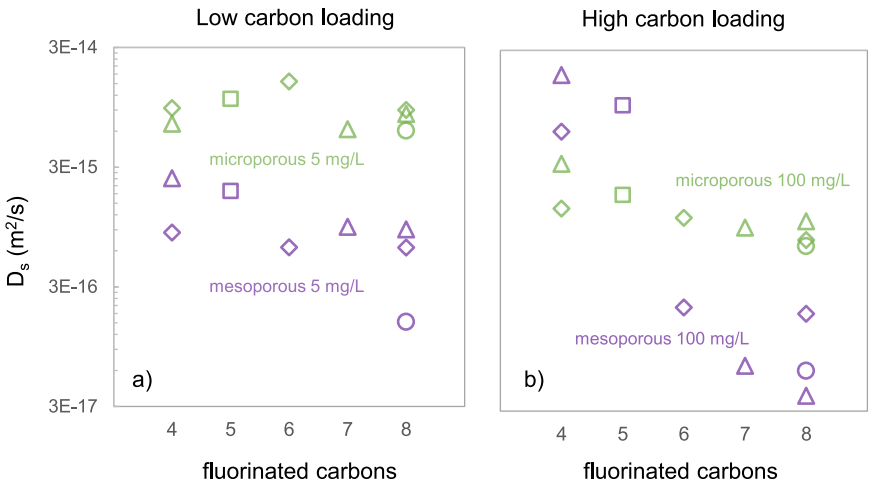

Fig. 4. Comparison of the estimated values of D_s for mesoporous SRD and microporous CS at a carbon dosage of 5 mg/L (a) and 100 mg/L (b), as a function of the PFAS chain length. The datapoints in the figure represent carboxylic PFAS (triangles), sulfonic PFAS (diamonds), GenX (squares), and FOSA (circles).

loadings due the greater total adsorption capacity of the activated carbon.

It has been observed that the molecular weight of adsorbates affects D_s with higher molecular weights resulting in lower D_s values (Worch, 2012). From our results this trend is the most clear in conditions with a lower PFAS surface saturation, as seen in Fig. 4. For instance, the impact of chain length on D_s is significantly more pronounced for SRD, which is less saturated with PFAS, than for CS at a carbon loading of 100 mg/L. Conditions of lower saturation may facilitate increased hydrophobic effects between the carbon surface and PFAS, and consequently have a stronger impact on the diffusion of longer-chain PFAS compared to conditions of higher saturation (e.g., CS at 100 mg/L). Moreover, at a lower carbon loading of 5 mg/L, the dependency of D_s on PFAS chain length for adsorption on CS 5 mg/L is not evident (Fig. 4a), likely due to the surface being fully saturated with PFAS, which minimizes PFAS-carbon interactions responsible for differentiation between long and short-chain PFAS.

To summarize this section, here D_s represents PFAS mobility on carbon surfaces, and is significantly influenced by interactions between PFAS molecules and the carbon material. Stronger interactions lead to a lower D_s. These interactions are more pronounced in mesoporous carbon compared to microporous carbon, as indicated by isotherm data, resulting in a lower D_s for mesoporous carbon. Additionally, higher saturation of the carbon surface with PFAS reduces these interactions, leading to an increase in D_s at lower carbon loadings. This observed behaviour, consistent with previous reports for other adsorbent/adsorbate systems (Worch, 2012; Do et al., 2001; Gilliland et al., 1974; Neretnieks, 1976a; Suzuki and Takao, 1982; Leyva-ramos, 2013; Neretnieks, 1976b), supports the conclusion that PFAS are likely transported by the mechanism of surface diffusion, even at low ng/L concentrations.

The estimated values of D_s for PFAS in this study, ranging from 10^{-14} to 10^{-17} m^2/s, are considerably lower than the commonly reported D_s values in literature, which typically range from 10^{-11} m^2/s for small molecules to 10^{-15} m^2/s for large molecules (Worch, 2012). A recent study by Dixit et al. (2021b) reported high D_s values of $\sim 10^{-9}$ m^2/s for PFAS adsorption on ion exchange resin in demineralized water at starting concentrations of PFAS of ~10 μg/L. However, values of D_s comparable to ours were obtained in a study by Burkhardt et al. (2022), by fitting isotherm parameters to model pilot-scale breakthrough curves. In our study and in Burkhardt et al., the lower D_s can probably by explained by the low PFAS concentrations in the ng/L range. The comparison with the study by Burkhardt et al. (2022) suggests that our experimentally based isotherm parameters can be used to accurately compute D_s values that can effectively predict the breakthrough curves in Burkhardt et al. (2022)

3.3. *Impact of isotherms at higher concentration on predicting PFAS adsorption at environmentally relevant concentration*

To evaluate the impact of isotherm parameters on the prediction of the surface diffusion coefficient (D_s), we obtained several isotherms for PFOA, at different initial concentrations, as shown in Fig. 5. Interestingly, Fig. 5 shows a strong dependence of the initial concentration on the amount of PFOA adsorbed (q_{eq}), at equivalent equilibrium concentrations (c_{eq}). For example, with microporous carbon at equilibrium concentrations between 10 and 20 ng/L, the adsorbed amount ranges from approximately 10 ng/L at a low initial PFOA concentration (~100 ng/L) to as much as 1000 ng/L at a higher initial concentration (~0.1 mg/L). This enhanced adsorption at higher starting concentrations could be attributed to multilayer adsorption involving PFAS aggregates, hemimicelles or micelles (Du et al., 2014; Zaggia et al., 2016; Mohona et al., 2023). Based on Fig. 5, it is clear that much of the isotherm data reported for PFOA in the literature should be interpreted with caution, as it may not accurately reflect PFOA adsorption behaviour at concentrations below 100 ng/L.

Several studies have conducted column experiments to investigate PFAS removal in the ng/L concentration range (Belkouteb et al., 2020; Chow et al., 2022; Liu et al., 2019). It would be valuable to describe the experimental data from those studies using a mechanistic column model that accounts for PFAS transport within the granule and adsorption (Worch, 2012). To employ such a model, isotherm parameters and diffusion coefficients obtained from this study are needed. Using isotherm parameters derived from high concentration experiments is an alternative, but these parameters fail to predict adsorption at low concentrations, as shown in Fig. 5. Moreover, high concentration-derived parameters cannot accurately determine diffusion coefficients at lower concentrations, as shown in Fig. 6. In this analysis, Freundlich parameters (Table S.21.) obtained at varying initial concentrations of PFOA were used to characterize the dynamics of an experiment with an initial concentration of 100 ng/L. For example, applying isotherm parameters derived from a 100 μg/L experiment to describe adsorption dynamics in the 100 ng/L range resulted in a calculated diffusion coefficient over 1000 times lower than when parameters determined within the 100 ng/L range were used. Thus, for accurate prediction in column experiments, it is essential to determine isotherm parameters and diffusion coefficients within the same concentration range.

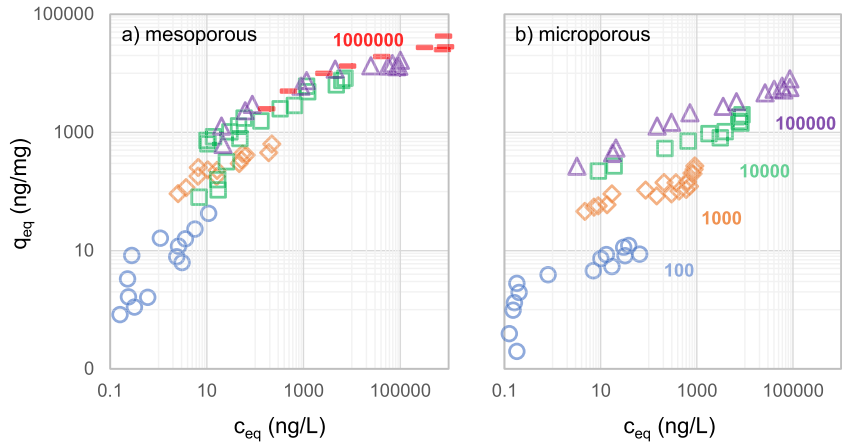

Fig. 5. PFOA adsorption equilibrium for SRD (a) and CS (b). Experimental data obtained for several PFOA concentration ranges with an initial concentration c_0 of ~ 100 ng/L (blue circles), c_0 ~ 1000 ng/L (orange diamonds), c_0 ~ 10 μg/L (green squares), c_0 ~ 100 μg/L (purple triangles), or c_0 ~ 1000 μg/L (red dashes).

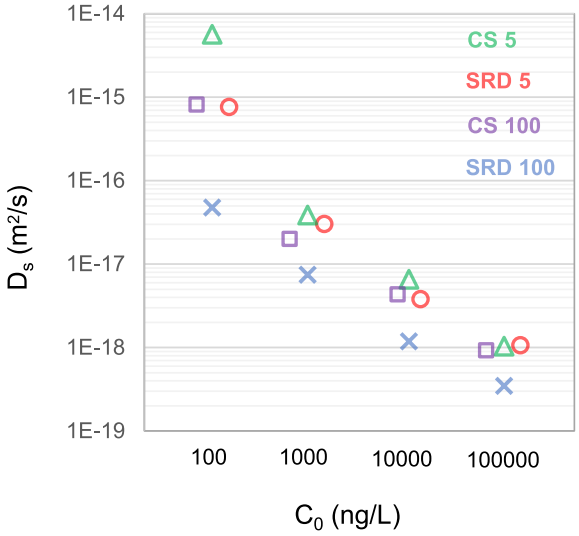

Fig. 6. Comparison of the estimated values of D_s (m^2/s) for mesoporous SRD and microporous CS at a carbon dosage of 5 mg/L and 100 mg/L for starting concentrations for which Freundlich isotherms were obtained and used to predict D_s.

4. Conclusion

We investigated the adsorption of nine distinct PFAS molecules at environmentally relevant concentrations of 0.1–100 ng/L onto two activated carbons with different pore size distributions. PFAS adsorption on microporous carbon exhibited saturation and was well described by the Langmuir isotherm, while adsorption on mesoporous carbon did not reach saturation and was better characterized by a linear isotherm. The unexpected saturation in microporous carbon at low PFAS concentrations suggests that micropores may play a less significant role in adsorbing both short- and long-chain PFAS compared to mesopores. When we compared our isotherm parameters with those reported in literature, we found that the Langmuir isotherm's maximum adsorption capacities were several orders of magnitude lower than previously reported. Our study focused on the low ng/L concentration range, whereas other studies were conducted at μg/L and mg/L levels. This discrepancy suggests that different PFAS adsorption mechanisms may operate at different concentrations, which requires further investigation. This hypothesis is further supported by our PFOA isotherm obtained at higher concentrations which showed a dependency on initial concentrations. Our findings also indicate that widely available adsorption data from high-concentration studies should be interpreted with caution, as our PFOA isotherms at high concentrations failed to accurately predict adsorption and kinetic behaviour at much lower concentrations of 0.1–100 ng/L.

To describe the intraparticle transport of PFAS, we coupled the estimated isotherms with surface and pore diffusion models. The experiments were conducted with both carbons at carbon dosages of 5 mg/L and 100 mg/L. Higher values of the surface diffusion coefficients (surface mobility) were observed for lower carbon loading when the surface was more saturated with PFAS, and when interactions between PFAS and carbon were expected to be weaker. Additionally, PFAS surface mobility in the more microporous carbon with lower adsorption capacity (higher PFAS surface saturation) were higher than in the more mesoporous carbon with higher adsorption capacity (lower PFAS surface saturation). These findings indicate that PFAS intraparticle mobility is a function of interactions between PFAS and carbon surface, where mobility decreases as the number or strength of interactions increases. Low values of the PFAS surface diffusion coefficients, particularly observed in carbons with a high number of active sites for adsorption, are an inherent limitation of heterogenous adsorbents such ase activated carbon, and deserves further investigation.

CRediT authorship contribution statement

Marko Pranić: Writing – review & editing, Writing – original draft, Visualization, Validation, Methodology, Conceptualization. **Livio Carlucci:** Writing – review & editing, Visualization, Validation, Methodology, Conceptualization. **Albert van der Wal:** Writing – review & editing, Visualization, Validation, Supervision, Methodology, Conceptualization. **Jouke E. Dykstra:** Writing – review & editing, Visualization, Validation, Supervision, Methodology, Conceptualization.

Declaration of competing interest

The authors declare that they have no known competing financial interests or personal relationships that could have appeared to influence the work reported in this paper.

Appendix A. Supplementary data

Supplementary data to this article can be found online at https://doi.org/10.1016/j.chemosphere.2024.143889.

Data availability

Data will be made available on request.

References

Ahrens, L., 2011. Polyfluoroalkyl compounds in the aquatic environment : a review of their occurrence and fate. J. Environ. Monit. 13 (20), 20–31. https://doi.org/10.1039/c0em00373e.

Appleman, T.D., Dickenson, E.R.V., Bellona, C., Higgins, C.P., 2013. Nanofiltration and granular activated carbon treatment of perfluoroalkyl acids. J. Hazard Mater. 260, 740–746. https://doi.org/10.1016/j.jhazmat.2013.06.033.

Ateia, M., Helbling, D.E., Dichtel, W.R., 2020. Best practices for evaluating new materials as adsorbents for water treatment. ACS Mater. Lett. 2 (11), 1532–1544. https://doi.org/10.1021/acsmaterialslett.0c00414.

Atkinson, A.J., Apul, O.G., Schneider, O., Garcia-Segura, S., Westerhoff, P., 2019. Nanobubble technologies offer opportunities to improve water treatment. Acc. Chem. Res. 52 (5), 1196–1205. https://doi.org/10.1021/acs.accounts.8b00606.

Belkouteb, N., Franke, V., McCleaf, P., Köhler, S., Ahrens, L., 2020. Removal of per- and polyfluoroalkyl substances (PFASs) in a full-scale drinking water treatment plant: long-term performance of granular activated carbon (GAC) and influence of flow-rate. Water Res. 182. https://doi.org/10.1016/j.watres.2020.115913.

Boone, J.S., Vigo, C., Boone, T., Byrne, C., Ferrario, J., Benson, R., Donohue, J., Simmons, J.E., Kolpin, D.W., Furlong, E.T., Glassmeyer, S.T., 2019. Per- and polyfluoroalkyl substances in source and treated drinking waters of the United States. Sci. Total Environ. 653, 359–369. https://doi.org/10.1016/j.scitotenv.2018.10.245.

Buck, R.C., Franklin, J., Berger, U., Conder, J.M., Cousins, I.T., Voogt, P. De, Jensen, A. A., Kannan, K., Mabury, S.A., van Leeuwen, S.P.J., 2011. Perfluoroalkyl and polyfluoroalkyl substances in the environment: terminology, classification, and origins. Integrated Environ. Assess. Manag. 7 (4), 513–541. https://doi.org/10.1002/ieam.258.

Burkhardt, J.B., Burns, N., Mobley, D., Pressman, J.G., Magnuson, M.L., Speth, T.F., 2022. Modeling PFAS removal using granular activated carbon for full-scale system design. J. Environ. Eng. 148 (3), 1–25. https://doi.org/10.1061/(asce)ee.1943-7870.0001964.

Cantoni, B., Turolla, A., Wellmitz, J., Ruhl, A.S., Antonelli, M., 2021. Perfluoroalkyl substances (PFAS) adsorption in drinking water by granular activated carbon: influence of activated carbon and PFAS characteristics. Sci. Total Environ. 795, 148821. https://doi.org/10.1016/j.scitotenv.2021.148821.

Chow, S.J., Croll, H.C., Ojeda, N., Klamerus, J., Capelle, R., Oppenheimer, J., Jacangelo, J.G., Schwab, K.J., Prasse, C., 2022. Comparative investigation of PFAS adsorption onto activated carbon and anion exchange resins during long-term operation of a pilot treatment plant. Water Res. 226, 119198. https://doi.org/10.1016/j.watres.2022.119198.

Dixit, F., Dutta, R., Barbeau, B., Berube, P., Mohseni, M., 2021a. PFAS removal by ion exchange resins: a review. Chemosphere 272, 129777. https://doi.org/10.1016/j.chemosphere.2021.129777.

Dixit, F., Barbeau, B., Lompe, K.M., Kheyrandish, A., Mohseni, M., 2021b. Performance of the HSDM to predict competitive uptake of PFAS, NOM and inorganic anions by suspended ion exchange processes. Environ. Sci. Water Res. Technol. 7 (8), 1417–1429. https://doi.org/10.1039/d1ew00145k.

Do, H.D., Do, D.D., Prasetyo, I., 2001. On the surface diffusion of hydrocarbons in microporous activated carbon. Chem. Eng. Sci. 56 (14), 4351–4368. https://doi.org/10.1016/S0009-2509(01)00051-3.

Du, Z., Deng, S., Bei, Y., Huang, Q., Wang, B., Huang, J., Yu, G., 2014. Adsorption behavior and mechanism of perfluorinated compounds on various adsorbents-A review. J. Hazard Mater. 274, 443–454. https://doi.org/10.1016/j.jhazmat.2014.04.038.

Du, Z., Deng, S., Chen, Y., Wang, B., Huang, J., Wang, Y., Yu, G., 2015. Removal of perfluorinated carboxylates from washing wastewater of perfluorooctanesulfonyl fluoride using activated carbons and resins. J. Hazard Mater. 286, 136–143. https://doi.org/10.1016/j.jhazmat.2014.12.037.

Franke, V., McCleaf, P., Lindegren, K., Ahrens, L., 2019. Efficient removal of per- and polyfluoroalkyl substances (PFASs) in drinking water treatment: nanofiltration combined with active carbon or anion exchange. Environ. Sci. Water Res. Technol. 5 (11), 1836–1843. https://doi.org/10.1039/c9ew00286c.

Gagliano, E., Sgroi, M., Falciglia, P.P., Vagliasindi, F.G.A., Roccaro, P., 2020. Removal of poly- and perfluoroalkyl substances (PFAS) from water by adsorption: role of PFAS chain length, effect of organic matter and challenges in adsorbent regeneration. Water Res. 171, 115381. https://doi.org/10.1016/j.watres.2019.115381.

Geankoplis, C.J., Leyva-Ramos, R., 1985. Model simulation and analysis of surface diffusion of liquids in porous solids. Chem. Eng. Sci. 40 (5), 799–807. https://doi.org/10.1016/0009-2509(85)85032-6.

Gebbink, W.A., Van Asseldonk, L., Van Leeuwen, S.P.J., 2017. Presence of emerging per- and polyfluoroalkyl substances (PFASs) in river and drinking water near a fluorochemical production plant in The Netherlands. Environ. Sci. Technol. 51 (19), 11057–11065. https://doi.org/10.1021/acs.est.7b02488.

Gilliland, E.R., Baddour, R.F., Perkinson, G.P., Sladek, K.J., 1974. Diffusion on surfaces. I. Effect of concentration on the diffusivity of physically adsorbed GAsses. Ind. Eng. Chem. Res. 13 (2), 95–100.

Gong, Y., Chen, Z., Bi, L., Kang, J., Zhang, X., Zhao, S., Wu, Y., Tong, Y., Shen, J., 2021. Adsorption property and mechanism of polyacrylate-divinylbenzene microspheres for removal of trace organic micropollutants from water. Sci. Total Environ. 781, 146635. https://doi.org/10.1016/j.scitotenv.2021.146635.

Higgins, C.P., Luthy, R.G., 2007. Modeling sorption of anionic surfactants onto sediment materials: an a priori approach for perfluoroalkyl surfactants and linear alkylbenzene sulfonates. Environ. Sci. Technol. 41 (9), 3254–3261. https://doi.org/10.1021/es062449j.

Inyang, M., Dickenson, E.R.V., 2017. The use of carbon adsorbents for the removal of perfluoroalkyl acids from potable reuse systems. Chemosphere 184, 168–175. https://doi.org/10.1016/j.chemosphere.2017.05.161.

Kancharla, S., Alexandridis, P., Tsianou, M., 2022. Sequestration of per- and polyfluoroalkyl substances (PFAS) by adsorption: surfactant and surface aspects. Curr. Opin. Colloid Interface Sci. 58, 101571. https://doi.org/10.1016/j.cocis.2022.101571.

Kaur, H., Bansiwal, A., Hippargi, G., Pophali, G.R., 2018. Effect of hydrophobicity of pharmaceuticals and personal care products for adsorption on activated carbon: adsorption isotherms, kinetics and mechanism. Environ. Sci. Pollut. Res. 25 (21), 20473–20485. https://doi.org/10.1007/s11356-017-0054-7.

KEMI, 2015. Occurrence and Use of Highly Fluorinated Substances and Alternatives Report from a Government Assignment. Swedish Chemicals Agency. Report 7/15.

Leyva-ramos, R., 2013. Role of Pore Volume and Surface Diffusion in the Adsorption of Aromatic Compounds on Activated Carbon 6, 945–957. https://doi.org/10.1007/s10450-013-9502-y.

Li, M., Sun, F., Shang, W., Zhang, X., Dong, W., Dong, Z., Zhao, S., 2021. Removal mechanisms of perfluorinated compounds (PFCs) by nanofiltration: roles of membrane-contaminant interactions. Chem. Eng. J., 406. https://doi.org/10.1016/j.cej.2020.126814.

Liu, C.J., Werner, D., Bellona, C., 2019. Removal of per- and polyfluoroalkyl substances (PFASs) from contaminated groundwater using granular activated carbon: a pilot-scale study with breakthrough modeling. Environ. Sci. Water Res. Technol. 5 (11), 1844–1853. https://doi.org/10.1039/c9ew00349e.

Liu, L., Liu, Y., Gao, B., Ji, R., Li, C., Wang, S., 2020. Removal of perfluorooctanoic acid (PFOA) and perfluorooctane sulfonate (PFOS) from water by carbonaceous nanomaterials: a review. Crit. Rev. Environ. Sci. Technol. 50 (22), 2379–2414. https://doi.org/10.1080/10643389.2019.1700751.

McNamara, J.D., Franco, R., Mimna, R., Zappa, L., 2018. Comparison of activated carbons for removal of perfluorinated compounds from drinking water. J. Am. Water Works Assoc. 110 (1), E2–E141. https://doi.org/10.5942/jawwa.2018.110.0003.

Mohona, T.M., Ye, Z., Dai, N., Nalam, P.C., 2023. Adsorption behavior of long-chain perfluoroalkyl substances on hydrophobic surface : a combined molecular characterization and simulation study. Water Res. 239, 120074. https://doi.org/10.1016/j.watres.2023.120074.

Neretnieks, I., 1976a. Analysis of some adsorption experiments with activated carbon. Chem. Eng. Sci. 31 (11), 1029–1035. https://doi.org/10.1016/0009-2509(76)87023-6.

Neretnieks, I., 1976b. Adsorption in finite bath and countercurrent flow with systems having a nonlinear isotherm. Chem. Eng. Sci. 31 (2), 107–114. https://doi.org/10.1016/0009-2509(76)85045-2.

Ochoa-Herrera, V., Sierra-Alvarez, R., 2008. Removal of perfluorinated surfactants by sorption onto granular activated carbon, zeolite and sludge. Chemosphere 72 (10), 1588–1593. https://doi.org/10.1016/j.chemosphere.2008.04.029.

Park, M., Wu, S., Lopez, I.J., Chang, J.Y., Karanfil, T., Snyder, S.A., 2020. Adsorption of perfluoroalkyl substances (PFAS) in groundwater by granular activated carbons: roles of hydrophobicity of PFAS and carbon characteristics. Water Res. 170. https://doi.org/10.1016/j.watres.2019.115364.

Piai, L., Dykstra, J.E., Adishakti, M.G., Blokland, M., Langenhoff, A.A.M., van der Wal, A., 2019. Diffusion of hydrophilic organic micropollutants in granular activated carbon with different pore sizes. Water Res. 162, 518–527. https://doi.org/10.1016/j.watres.2019.06.012.

Qiu, Y., Fujii, S., Tanaka, S., 2007. Removal of perfluorochemicals from wastewater by granular activated carbon adsorption. Environmeantal Eng. Res. 44 (23), 185–193. https://doi.org/10.11532/proes1992.44.185.

Roest, K., ter Laak, T.L., Huiting, H., Siegers, W., Meekel, N., Jong, C. de, Jong, M. de, Houten, M. van, Pancras, T., Plaisier, W., Dalmijn, J., 2021. Performance of water treatment systems for PFAS removal. Concawe Rep. (5/21).

Schrenk, D., Bignami, M., Bodin, L., Chipman, J.K., del Mazo, J., Grasl-Kraupp, B., Hogstrand, C., Hoogenboom, L., Leblanc, J.C., Nebbia, C.S., Nielsen, E., Ntzani, E., Petersen, A., Sand, S., Vleminckx, C., Wallace, H., Barregård, L., Ceccatelli, S., Cravedi, J.P., Halldorsson, T.I., Haug, L.S., Johansson, N., Knutsen, H.K., Rose, M., Roudot, A.C., Van Loveren, H., Vollmer, G., Mackay, K., Riolo, F., Schwerdtle, T., 2020. Risk to human health related to the presence of perfluoroalkyl substances in Food. EFSA J. 18 (9). https://doi.org/10.2903/j.efsa.2020.6223.

Sörengård, M., Östblom, E., Köhler, S., Ahrens, L., 2020. Adsorption behavior of per- and polyfluoralkyl substances (PFASs) to 44 inorganic and organic sorbents and use of dyes as proxies for PFAS sorption. J. Environ. Chem. Eng. 8 (3), 103744. https://doi.org/10.1016/j.jece.2020.103744.

Souza, P.R., Dotto, G.L., Salau, N.P.G., 2017. Detailed numerical solution of pore volume and surface diffusion model in adsorption systems. Chem. Eng. Res. Des. 122, 298–307. https://doi.org/10.1016/j.cherd.2017.04.021.

Suzuki, M., Takao, F., 1982. Concentration dependence of surface diffusion coefficient of propionic acid in activated carbon particles. AIChE J. 28 (3), 380–385. https://doi.org/10.1002/aic.690280303.

The European Parliament and the Council of the European Union, 2020. Directive (EU) 2020/2184. Off. J. Eur. Union L 435/1.

The European Parliament and the Council of the European Union, 2022. Proposal for a Directive 2022/0344 (COD).

US EPA, 2024. National Primary Drinking Water Regulation.

Vakili, M., Bao, Y., Gholami, F., Gholami, Z., Deng, S., Wang, W., Kumar Awasthi, A., Rafatullah, M., Cagnetta, G., Yu, G., 2021. Removal of HFPO-da (GenX) from aqueous solutions: a mini-review. Chem. Eng. J. 424, 130266. https://doi.org/10.1016/j.cej.2021.130266.

Worch, E., 2012. Adsorption technology in water treatment. https://doi.org/10.1515/9783110240238.

Wu, C., Klemes, M.J., Trang, B., Dichtel, W.R., Helbling, D.E., 2020. Exploring the factors that influence the adsorption of anionic PFAS on conventional and emerging adsorbents in aquatic matrices. Water Res. 182, 115950. https://doi.org/10.1016/j.watres.2020.115950.

Yu, Q., Zhang, R., Deng, S., Huang, J., Yu, G., 2009. Sorption of perfluorooctane sulfonate and perfluorooctanoate on activated carbons and resin: kinetic and isotherm study. Water Res. 43 (4), 1150–1158. https://doi.org/10.1016/j.watres.2008.12.001.

Yu, J., Lv, L., Lan, P., Zhang, S., Pan, B., Zhang, W., 2012. Effect of effluent organic matter on the adsorption of perfluorinated compounds onto activated carbon. J. Hazard Mater. 225–226, 99–106. https://doi.org/10.1016/j.jhazmat.2012.04.073.

Yuan, S., Wang, X., Jiang, Z., Zhang, H., Yuan, S., 2023. Contribution of air-water interface in removing PFAS from drinking water: adsorption, stability, interaction and machine learning studies. Water Res. 236, 119947. https://doi.org/10.1016/j.watres.2023.119947.

Zaggia, A., Conte, L., Falletti, L., Fant, M., Chiorboli, A., 2016. Use of strong anion exchange resins for the removal of perfluoroalkylated substances from contaminated drinking water in batch and continuous pilot plants. Water Res. 91, 137–146. https://doi.org/10.1016/j.watres.2015.12.039.